Journal of Global Change Data & Discovery. 2022, 6(4): 545-556
www.geodoi.ac.cn

Global High-temperature Disaster Risk of Rice Dataset

Su, P.[1,3] Wang, J. A.[1,2*] Zhang, A. Y.[1] Wang, R.[1]

1. Faculty of Geographical Science, Beijing Normal University, Beijing 100875, China;
2. Key Laboratory of Tibetan Plateau Land Surface Processes and Ecological Conservation (Ministry of Education), Xining 810008, China;
3. China School of Geographic Science, Qinghai Normal University, Xining 810008, China

Abstract: Under the background of climate change and population expansion, the food supply pressure increased. Rice is a temperature-sensitive crop, thus its future yield and growth environment will also undergo significant changes with climate changes. This paper used the MaxEnt model and the redistribution method to project the planting areas under rice. Through combining the planting area and extreme high temperature disasters, we obtained the high–temperature exposure to rice. The EPIC model was used to generate the vulnerability curve of rice yield loss responding to high-temperature stress. In addition, the yield loss rate under different scenarios obtained by high-temperature intensity and vulnerability curves. It was treated as the rice yield loss data. The dataset was divided into three parts, rice potential cultivation area data, rice high–temperature exposure data, and rice high-temperature yield loss data. The spatial resolution of the rice potential cultivation area data and rice high-temperature exposure data is 0.25°×0.25° , and the spatial resolution of rice high-temperature yield loss data is 0.5°×0.5°. The dataset consisted of 21 files in total, and the data size was about 46.8MB.

Keywords: global change; rice; crop potential distribution; exposure; vulnerability

DOI: https://doi.org/10.3974/geodp.2022.04.05

CSTR: https://cstr.escience.org.cn/CSTR:20146.14.2022.04.05

Dataset Availability Statement:

The dataset supporting this paper was published and is accessible through the *Digital Journal of Global Change Data Repository* at: https://doi.org/10.3974/geodb.2022.06.04.V1 or https://cstr.escience.org.cn/CSTR:20146.112022.06.04.V1.

1 Introduction

The latest IPCC special report pointed out that according to the current global warming rate, the global temperature will rise by 1.5 ℃ by 2040[1], which will change the growth environment of rice in the future. Without considering the improvement of crops varieties,

Received: 10-07-2022; **Accepted:** 30-11-2022; **Published:** 24-12-2022

Foundation: Ministry of Science and Technology of P. R. China (2016YFA0602402)

***Corresponding Author:** Wang, J. A. AAA-6406-2022, Faculty of Geographical Science, Beijing Normal University, jwang@bnu.edu.cn

Data Citation: [1] Su, P., Wang, J. A., Zhang, A. Y., *et al*. Global high–temperature disaster risk of rice dataset [J]. *Journal of Global Change Data & Discovery*, 2022, 6(4): 545–556. https://doi.org/10.3974/geodp.2022.04.05. https://cstr.escience.org.cn/CSTR:20146.14.2022.04.05.

[2] Su, P., Wang, J. A., Zhang, A. Y., *et al*. Global rice high-temperature disaster risk simulating dataset (2030s, 2050s) [J/DB/OL]. *Digital Journal of Global Change Data Repository*, 2022. https://doi.org/10.3974/geodb.2022.06.04.V1 or https://cstr.escience.org.cn/CSTR:20146.112022.06.04.V1.

the cultivation area of rice in the future should be adjusted to the environment. Similarly, the global high–temperature disasters on rice will also undergo spatial and temporal changes in the future, which necessitate crop distribution, exposure and yield loss data –for rice. Therefore, we can intuitively recognize the distribution of rice planting area and the yield loss induced by extreme high–temperature under different scenarios, which helps to formulate measures to reduce losses according to local conditions[2], and it is of great significance to world food security.

2 Metadata of the Dataset

The metadata of the Global rice high-temperature disaster risk simulating dataset (2030s, 2050s)[3] is summarized in Table 1. It includes the dataset full name, short name, authors, year of the dataset, temporal resolution, spatial resolution, data format, data size, data files, data publisher, and data sharing policy, etc.

Table 1 Metadata summary of the Global rice high-temperature disaster risk simulating dataset (2030s, 2050s)

Items	Description
Dataset full name	Global rice high-temperature disaster risk simulating dataset (2030s, 2050s)
Dataset short name	GlobalRiceRisk
Authors	Wang, J. A. AAA–6406–2022, Faculty of Geographical Science, Beijing Normal University, and Key Laboratory of Tibetan Plateau Land Surface Processes and Ecological Conservation (Ministry of Education), jwang@bnu.edu.cn Su, P. ABH–3399–2021, School of Geographic Science, Qinghai Normal University, 201947331031@stu.qhnu.edu.cn Zhang, A. Y. AAA–6787–2022, Faculty of Geographical Science, Beijing Normal University, zay@mail.bnu.edu.cn Wang, R. AAE–1120–2019, Faculty of Geographical Science, Beijing Normal University, wangr0225@163.com
Geographical region	Global
Year	2000s, 2030s and 2050s
Temporal resolution	1970–2000 (2000s), 2016–2035 (2030s) and 2046–2065 (2050s)）
Spatial resolution	The spatial resolution of rice distribution and exposure data is 0.25°×0.25°, and the spatial resolution of rice vulnerability data is 0.5°×0.5°
Data format	.tif
Data size	46.8 MB
Data files	Rice cultivation area data, rice high-temperature exposure data, and rice high–temperature vulnerability data
Foundation	Ministry of Science and Technology of P. R. China (2016YFA0602402)
Data publisher	Global Change Research Data Publishing & Repository, http://www.geodoi.ac.cn
Address	No. 11A, Datun Road, Chaoyang District, Beijing 100101, China
Data sharing policy	***Data*** from the Global Change Research Data Publishing & Repository includes metadata, datasets (in the *Digital Journal of Global Change Data Repository*), and publications (in the *Journal of Global Change Data & Discovery*). ***Data*** sharing policy includes: (1) ***Data*** are openly available and can be free downloaded via the Internet; (2) End users are encouraged to use ***Data*** subject to citation; (3) Users, who are by definition also value–added service providers, are welcome to redistribute ***Data*** subject to written permission from the GCdataPR Editorial Office and the issuance of a ***Data*** redistribution license; and (4) If ***Data*** are used to compile new datasets, the 'ten per cent principal' should be followed such that ***Data*** records utilized should not surpass 10% of the new dataset contents, while sources should be clearly noted in suitable places in the new dataset[4]
Communication and searchable system	DOI, CSTR, Crossref, DCI, CSCD, CNKI, SciEngine, WDS/ISC, GEOSS

3 Methods

3.1 Data Collection or Processing

The original data used in this study, including environment data (topographic and soil properties data), crop data (historical rice planting area data) and scenarios data (climate data). This paper selected the global digital elevation model (DEM) from USGS and the global surface slope data of GAEZ as topographic data. This paper selected global soil properties data from ISRIC. The historical rice harvested area data came from EARTHSTAT, SPAM 2005 v2.0, and MIRCA2000. The climate data in this paper were from NASA, including precipitation, the highest temperature and the lowest temperature. And the multi-mode data results are averaged to get the comprehensive results. The detailed data list is shown in Table 2.

Table 2 Database information

Category	Name	Year	Temporal Resolution	Sources
Environ-ment data	Global Multi–resolution Terrain Elevation Data (GMTED2010)	2010	1 km×1 km	United States Geological Survey (USGS) https://topotools.cr.usgs.gov/gmted_viewer/
	WISE derived soil properties on a 30 by 30 arc–seconds global grid	2012	30″×30″	International Soil Reference and Information Centre (ISRIC) http://www.isric.org
Crop data	①Harvested Area and Yield for 175 Crops year 2000 ②SPAM 2005 v2.0 ③MIRCA2000	2000 or 2005	5′×5′	①http://www.earthstat.org/harvested–area–yield–175–crops/ ②http://mapspam.info/maps/ ③http://www.uni–frankfurt.de/45218031/data_download?
	FAO rice production statistics	1960–2015	Country unit and subnational unit	http://www.fao.org/faostat/en/#data/QC; http://kids.fao.org/agromaps/
	FAO rice demand statistics	1960–2015	Country unit	http://www.fao.org/faostat/en/#data/FBS
	FAO demographic data	1960–2015	Country unit	http://www.fao.org/faostat/en/#data/OA
	FAO GDP statistics	1960–2015	Country unit	http://www.fao.org/faostat/en/?#data/MK
	Rice growth period	1961–1990	5′×5′	https://nelson.wisc.edu/sage/data–and–models/crop–calendar–dataset/index.php
Scenarios data	NASA's Climate Data Services	1960–2099	0.25°×0.25°	https://cds.nccs.nasa.gov/nex–gddp/
	Global dataset of gridded population and GDP scenarios	2005–2099	0.25°×0.25°	http://www.cger.nies.go.jp/gcp/population–and–gdp.html
	Land–Use Harmonization 2 (LUH2)	1970–2100	0.25°×0.25°	http://luh.umd.edu/data.shtml
	Historical wind speed (WorldClim V1.4)	1970–2000	5′×5′	http://www.worldclim.com/version1
	Wind speed under different scenarios	1970–2099	0.5°×0.5°	https://www.isimip.org/gettingstarted/input–data–bias–correction/

3.2 Methodology

3.2.1 Estimated Rice Cultivation Distribution

3.2.1.1 Estimated Potential Distribution of Rice

This dataset used the MaxEnt model to estimate rice potential distributions. This model is

based on the maximum entropy method to simulate the species niche and distribution. The input data of the model were the crop distribution samples and the environmental variables. Refer to the previous work[5], the selection of samples and environmental variables in this paper showed as follows.

First, we calculated the ratio of historical crop cultivation area. Secondly, we divided the ratio into four groups, and the fourth group (ratio≥66%) determined the number of samples selected in the other three groups according to the proportion of the cultivation area and the number of samples. Besides, we used the randperm function in MATLAB to randomly select the specified number of samples in each group. The number of samples was 559 (ratio <10%), 768 (10%≤ratio <33%), 541 (33%≤ratio <66%) and 360 (66%≤ratio).

In order to reduce the impact of random selection of samples, this paper chose 30 sets of samples. We calculated rice suitability by these 30 sets of samples, and took the averaged results as the final rice suitability.

This study believed that terrain, climate[6–8] and soil[9–11], topography were the factors that affected rice growth. Hence, we chose elevation, climate indicators (22 indicators) and soil indicators (20 indicators) as candidate indicators[12]. In order to extract indicators with a significant impact on the growth range of rice, we screened the indicators three times. See Table 3 for the indicators used in the model.

Table 3 The indicators used in MaxEnt model

Data	Indicators	Meaning of indicators
Climate	BIO1	Annual mean temperature
	BIO2	Mean diurnal range
	BIO3	Isothermality
	BIO5	Max temperature of warmest month
	BIO8	Mean temperature of wettest quarter
	BIO12	Annual precipitation
	BIO18	Precipitation of warmest quarter
	Solar radiation	Solar radiation
	Wind speed	Wind speed
Soil	CECS	Cation exchange capacity
	CFRAG	Coarse fragments % (> 2 mm)
	CNrt	C/N ratio
	GYPS	Gypsum content
	ORGC	Organic carbon content
	TAWC	Volumetric water content
	TEB	Total exchangeable bases
Topography	DEM	digital elevation model (DEM)

3.2.1.2 Estimated Rice Yield Redistribution

(1) Rice yield estimation

The relationship between per capita rice demand and per capita GDP was used to calculate the amount of rice consumption under different SSP scenario. The fitting function referred to previous research mainly including power function linear model[13] and logarithmic linear model[14] (see Figure 1 for fitting examples). An example of curve fitting of per capita GDP and per capita rice demand was shown in the figure 1.

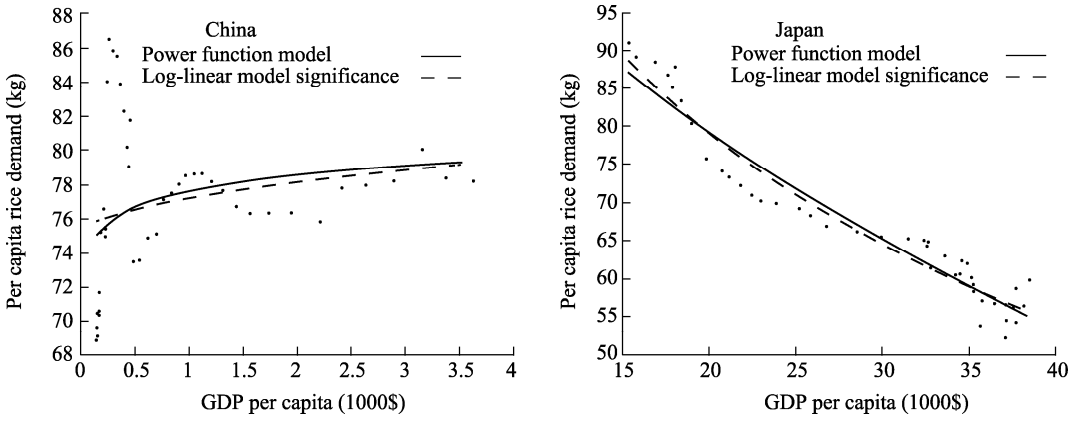

Figure 1 Curve fitting of GDP per capita and per capita annual rice demand

(2) Rice yield redistribution

The overall idea of redistribution of rice yield can be expressed as a multi-objective optimization model where equations 1–4 are established at the same time.

$$D = S + I \tag{1}$$

where, D, S and I represent the country's rice demand, supply and net import respectively.

$$A_{i,\text{rice}} \leqslant A_{i,c3} \tag{2}$$

where, $A_{i,\text{rice}}$ and $A_{i,c3}$ represent the rice harvest area and C3 crop harvest area of the *i*–th grid, respectively.

$$\sum (A_{i,n+1} \cdot Su_i) \geqslant \sum (A_{i,n} \cdot Su_i)(n = 1, 2, 3\ldots) \tag{3}$$

where, n represents the number of iterations, n=1 represents the initial situation inferred from the change in the suitable zone, and *Su* represents the suitability.

$$Ir_{FAO} = \frac{\sum A_{i,Ir}}{\sum A_{i,rice}} \tag{4}$$

where, Ir_{FAO} represents the national rice irrigation rate predicted by FAO, and $A_{i,Ir}$ and $A_{i,rice}$ represent the rice irrigation area and rice harvest area in grid i, respectively.

When adjusting the rice harvest area, we followed the following three principles: (1) make the country's rice supply and demand balance; (2) make the country's rice irrigation ratio as close as possible to the FAO forecast value; (3) when increasing (or decreasing) the planting area, start from the high suitable area (or start to decrease from the low suitable area), until the rice is planted to all the cultivated land in the suitable area (or there is no rice planted). Since it is impossible to determine the irrigation ratio within the increase range, it is assumed that the irrigation ratio for all the increased areas is the same. Figure 2 showed the process in detail.

3.2.2 Exposure and Vulnerability Estimation Methods

3.2.2.1 Calculation of Hazard

The rice exposure to high–temperature was calculated by the high temperature days and the accumulated temperature exceeding the rice growth threshold. The rice growth threshold was defined as the maximum temperature suitable for rice growth during the rice growth period[15] (the growth threshold of rice is 38 ℃). We defined a single-day average

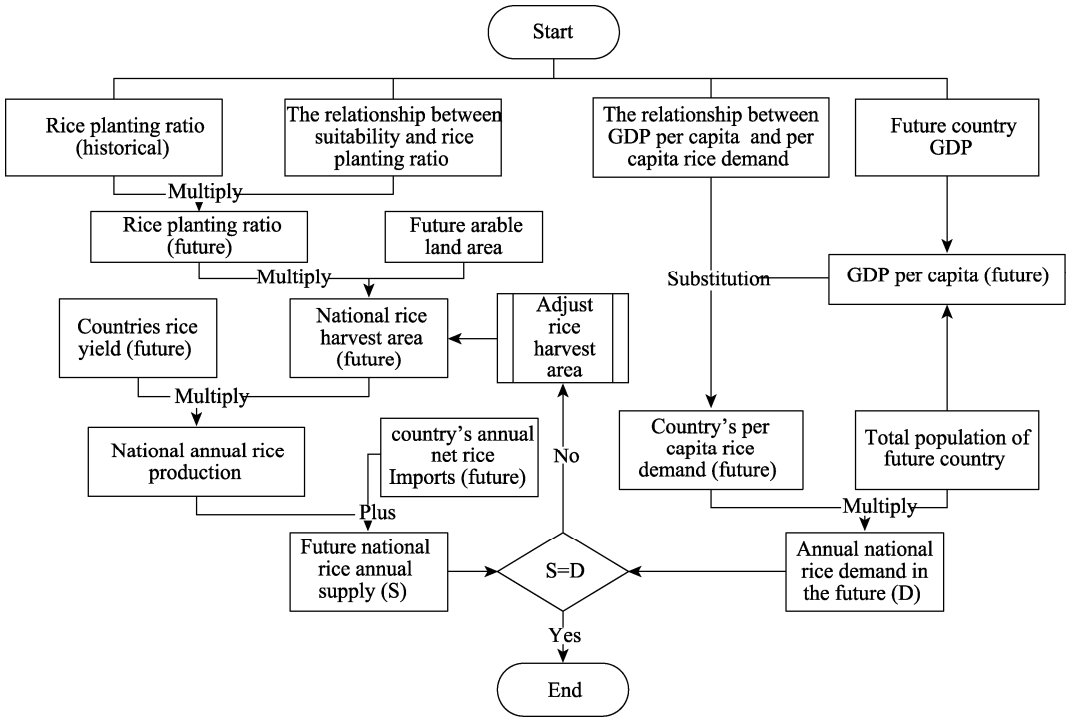

Figure 2 The future rice harvest area and yield estimation framework

temperature exceeding 38 ℃ (≥38 ℃) as a high-temperature event for rice, and used the cumulative stress value (GHTS) of the high-temperature event during the growth period as the high–temperature intensity.

3.2.2.2 Calculation of Rice Exposure

The exposure of rice is the spatial superposition of the rice potential distribution area and the hazard area. The exposure indicators used in this dataset were the rice harvest area.

3.2.2.3 Calculation of Rice Vulnerability

The vulnerability curve is established through binary relationship between the intensity of the hazard and the loss of the crop. In this study, the EPIC model was used to construct the vulnerability curve of rice through the high-temperature intensity and yield loss rate. According to the vulnerability curve and the high-temperature intensity under different scenarios, the loss rate of rice under each scenario was obtained.

The EPIC model is a dynamic model that integrates factors such as climate, soil, moisture, and field management, and is often used for crop yield simulation. This paper used the EPIC model to calculate the vulnerability curve between the high-temperature intensity and the rice yield loss rate. The equations are as follows.

The high temperature disaster intensity index (*HSI*) in this study was defined as

$$TS = \sum_{i=1}^{n} (1 - TS_i)$$
$$HSI = \frac{TS}{TS_{max}} \quad (5)$$

where, TS_i represents the temperature stress value on the *i–th* day, *n* represents the number of days during the growth period, *TS* represents the cumulative temperature stress during the growth period under a certain scenario, and TS_{max} represents the potential maximum value of

the cumulative stress during the growth period.

The yield loss rate (*YL*) in this study was defined as

$$YL = \frac{Y_{max} - Y}{Y_{max}} \times 100\% \tag{6}$$

where, *Y* represents the simulated output under a certain scenario, and Y_{max} represents the simulated output under the optimal scenario (*TS*=0).

According to the above equations, the *HSI* and the corresponding *YL* were used to fit the vulnerability curve through the logistics regression equation. The fitting equation used in this study was:

$$YL = \frac{(a/(1+b\times exp\,(c\times HSI)) - a/(1+b))}{(a/(1+b\times exp\,(c)) - a/(1+b))} \times d \tag{7}$$

where, *a*, *b*, *c*, *d* are curve function parameters.

3.2.2.4 Calculation of Rice Yield Loss

In the exposed area, the probability density curve of the high-temperature disaster intensity was calculated by using the information diffusion theory, and combined it with the vulnerability curve, the probability density curve of the rice yield loss rate was obtained. Then, we calculated its loss expectation to reflect the average state of rice yield loss induced by high temperature disasters.

The cumulative high-temperature stress value in a certain period was simulated by EPIC, and the annual high-temperature disaster intensity index (HSI) was calculated (Equation 5). Taking this data as an information diffusion sample, the probability density distribution was estimated by using the normal diffusion method. The specific calculation process is as follows:

Let $U=\{u_1, u_2,\ldots,u_n\}$ be the discrete universe containing the possible values of HSI, the value range of HSI is 0 to 1, and the resolution of the universe is 0.0001, so $U=\{0,0.0001,0.0002,\ldots,1\}$. The information carried by the HSI in each grid is diffused into each u_i through the information diffusion function (Equation 8).

$$f_k(u_i) = \frac{1}{h\sqrt{2\pi}} \times exp\left[-\frac{(HSI_k - u_i)^2}{2h^2}\right] \tag{8}$$

where, *k* is the code of each grid, *h* is the normal diffusion coefficient, which can be calculated by Equation 9.

$$h = \begin{cases} 0.8146(b-a), & m=5 \\ 0.5960(b-a), & m=6 \\ 0.4560(b-a), & m=7 \\ 0.3860(b-a), & m=8 \\ 0.3362(b-a), & m=9 \\ 0.2986(b-a), & m=10 \\ 2.8651\dfrac{b-a}{n-1}, & m \geqslant 11 \end{cases} \tag{9}$$

where *a* and *b* are the minimum and maximum values of HSI, respectively, and *m* is the number of samples. Then the information accumulation and normal information distribution of the sample can be calculated by Equation 10 and Equation 11, respectively.

$$C_k = \sum_{i=1}^{n} f_k(u_i) \tag{10}$$

$$F(HSI_k, u_j) = \frac{f_k(u_i)}{C_k} \tag{11}$$

where, C_k is the information accumulation of each k^{th} sample, $F(HSI_k, u_j)$ is the normalized information distribution of HSI, for each point u_j, add all normalized information to get the HSI from the given sample at u_j information gain. The information gain is shown in Equation 12.

$$q(u_j) = \sum_{j=1}^{m} F(HSI_i, u_j) \tag{12}$$

The diffusion information of the sample was obtained by summing $q(u_i)$ (Equation 13):

$$Q = \sum_{i=1}^{n} q(u_i) \tag{13}$$

Then calculated the probability density distribution of HSI (Equation 14):

$$p(u_i) = \frac{q(u_i)}{Q} \tag{14}$$

Defined the probability density distribution of HSI as the expected value of the yield loss rate of rice in a certain period (Equation 15).

$$E = \sum [p(u_j) \times u_j] \tag{15}$$

where, $p(u_j)$ is the estimated probability value when the high-temperature disaster intensity is u_j.

3.3 Technical Route

The dataset was divided into three parts: rice potential cultivation area data, rice high-temperature exposure data, and rice yield loss data. Among them, the rice potential cultivation area data was calculated under the natural and socio-economic scenarios, the rice high-temperature exposure data was calculated by the hazard and the rice planting area. The rice yield loss data was calculated from the rice vulnerability curve, which was simulated by the EPIC model. The detailed process was shown in Figure 3.

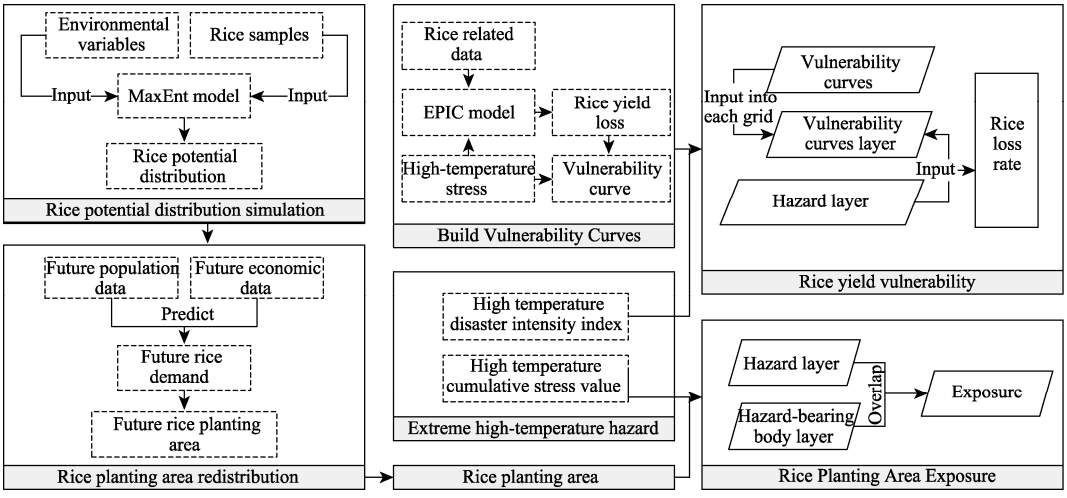

Figure 3 Data producing technical route

4 Data Results and Validation

4.1 Data Composition

The dataset was divided into 1970–2000 (historical), 2016–2035 (near-term), and 2046–2065 (mid-term). The scenarios were divided into three combinations of rcp2.6–ssp1, rcp4.5–ssp2 and rcp8.5–ssp3.

Data spatial resolution: The spatial resolution of rice distribution and exposure data is 0.25°×0.25°, and the spatial resolution of rice vulnerability data is 0.5°×0.5°.

Data format: GeoTIFF.

4.2 Data Products

4.2.1 Display of Rice Cultivation Area Data

In this paper, the MaxEnt model was used to simulate the natural suitable areas of rice, and on this basis, the supply and demand allocation of national units was carried out, and finally the rice planting area under different scenarios was obtained and mapped (Figure 4). Compared with the historical period, under the RCP8.5–SSP3 scenario, the planting area of rice in mid-term showed a decreasing trend, with the most obvious decrease in planting area in South America and the Indian peninsula.

4.2.2 Display of Rice High-temperature Exposure Data

The rice planting area and the extreme high-temperature hazard area were superimposed to obtain the rice exposure to high-temperature under each scenario, and mapped (Figure 5). Compared with the historical period, under the RCP8.5–SSP3 scenario, the area of rice exposure to high temperature will generally increase in the mid-term, with the most significantly in Africa and southern China.

4.2.3 Display of Rice High-temperature Vulnerability Data

Combining the rice vulnerability curve with the high-temperature hazard, the yield loss ratio of rice caused by high-temperature under each scenario was obtained and mapped (Figure 6). Compared with the historical period, under the RCP8.5–SSP3 scenario, the loss of rice in the mid-term increased significantly.

4.3 Data Validation

This dataset was calculated based on hazard (high temperature events) and hazard bearing body (rice planting area). The hazard was calculated from different climatic models from CMIP5. The availability of these data has been widely proven[16]. The calculation processes of rice planting area were divided into rice potential distribution and rice planting redistribution. The process of redistribution was based on the historical rice harvest data, so it is difficult to verify its accuracy. Therefore, the accuracy verification of this dataset mainly focused on the verification of the rice potential distribution. In the previous research, we verified the suitable area by remote sensing image classification and other methods[6], which proved the rationality of the data. Here we would discuss the random selection of samples in more details.

When the number of random sample groups was more than 30, the uncertainty reduction was not significant. Therefore, considering the reduction of uncertainty and efficiency, we

chose to set the number of sample groups to 30. The standard deviations of 30 random sample groups were spatially mapped, as shown in Figure 7.

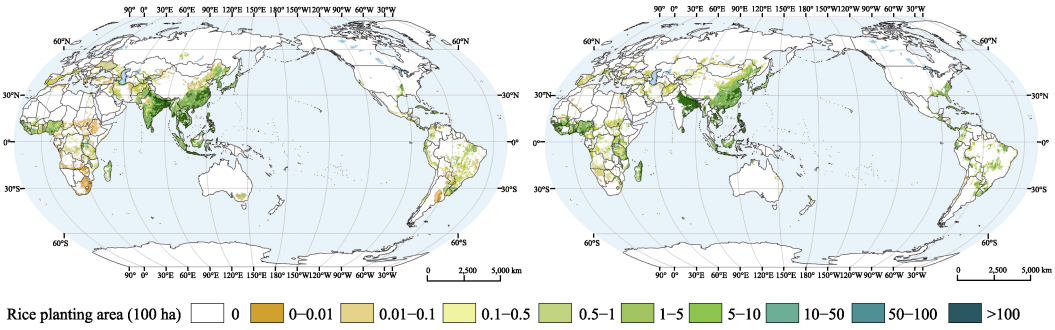

(a) The historical distribution map (b) Mid-term under RCP8.5–SSP3 scenario map

Figure 4 Rice planting distribution of historical period and mid-term under the RCP8.5–SSP3 scenario

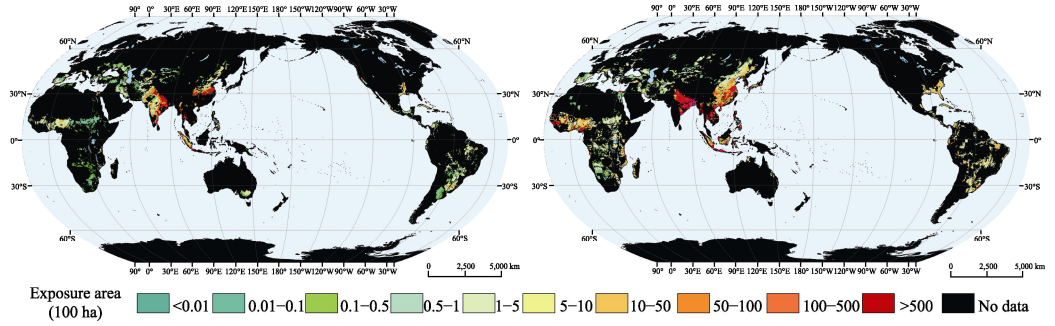

(a) The historical distribution map (b) Mid-term under RCP8.5–SSP3 scenario map

Figure 5 Map of rice exposure to extreme high temperature hazard

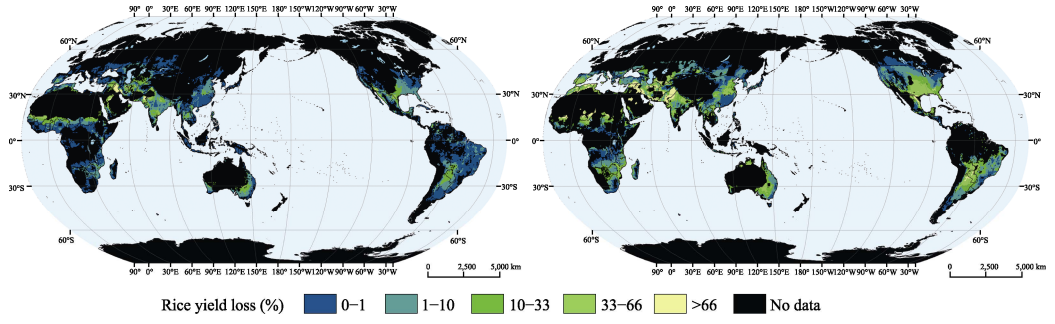

(a) The historical distribution map (b) Mid-term under RCP8.5–SSP3 scenario map

Figure 6 Map of Rice yield loss caused by high-temperature hazard

The figure showed that the areas with large standard deviations were mainly concentrated in the Pamirs and Asia Minor Peninsula, indicating that the simulation results of rice distribution in these regions were quite different among the sample groups. Due to historical rice planting area in these two regions was relatively small, so it had little effect on the overall simulation results.

5 Discussion and Conclusion

This dataset used the MaxEnt model and redistribution method to obtained the distribution of rice planting. Through remote sensing classification, ROC curve and other methods, this paper verified the validity of the rice distribution prediction. By calculating the hazed intensity caused by future high temperature event, and combined it with the crop distribution, we obtained rice exposure to high-temperature data. Using the EPIC model to simulate the yield loss rate of rice under different intensities of high temperature stress, we obtained the vulnerability curve of rice facing high-temperature hazard, and then we obtained the rice yield loss rate.

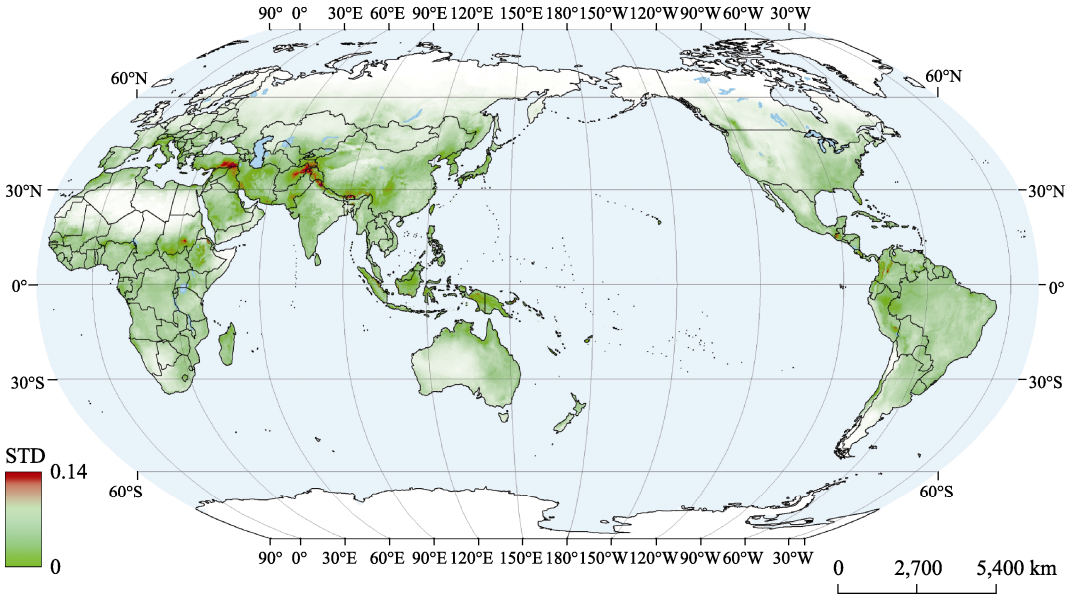

Figure 7 Map of spatial distribution of standard deviations (30 sample groups)

This dataset comprehensively considered the impacts of the natural and socio-economic factors to estimate the future rice planting distribution. On this basis, we calculated exposure and vulnerability with consideration the dual dynamic changes of crop and hazard. On the one hand, this dataset has significance for future rice planting and food security research. On the other hand, it also has important value for climate change impact assessment.

Author Contributions

Wang, J. A. designed the algorithms of dataset. Zhang, A. Y. and Wang, R. contributed to the data processing and analysis. Su, P., Zhang, A. Y. and Wang, R. contributed to the measures. Su, P. contributed to the data verification.

Conflicts of Interest

The authors declare no conflicts of interest.

References

[1] Intergovernmental Panel on Climate Change. Global warming of 1.5 ℃ [R]. Geneva, Switzerland: World Meteorological Organization, 2018.

[2] Fraser, S., Wood, N., Johnston, D., *et al*. Variable population exposure and distributed travel speeds in least–cost tsunami evacuation modeling [J]. *Natural Hazards and Earth System Sciences*, 2014, 2(6): 4163–4200.

[3] Su, P., Wang, J. A., Zhang, A. Y., *et al*. Global rice high-temperature disaster risk simulating dataset (2030s, 2050s) [J/DB/OL]. *Digital Journal of Global Change Data Repository*, 2022. https://doi.org/10.3974/geodb.2022.06.04.V1. https://cstr.escience.org.cn/CSTR:20146.112022.06.04.V1.

[4] GCdataPR Editorial Office. GCdataPR data sharing policy [OL]. https://doi.org/10.3974/dp.policy.2014.05 (Updated 2017).

[5] Su, P., Zhang, A., Wang, R., *et al.* Prediction of future natural suitable areas for rice under representative concentration pathways (RCPs) [J]. *Sustainability*, 2021, 13(3): 1580.

[6] Yoshida, S., Parao, F. T. Climatic influence on yield and yield components of lowland rice in the tropics [J]. *Climate and Rice*, 1976, 20: 471–494.

[7] Lobell, D. B., Schlenker, W., Costa–Roberts, J. Climate trends and global crop production since 1980 [J]. *Science*, 2011, 333(6042): 616–620.

[8] Lobell, D. B., Gourdji, S. M. The influence of climate change on global crop productivity [J]. *Plant physiology*, 2012, 160(4): 1686–1697.

[9] Azam, F. Comparative effects of organic and inorganic nitrogen sources applied to a flooded soil on rice yield and availability of N [J]. *Plant & Soil*, 1990, 125(2): 255–262.

[10] Kravchenko, A. N., Bullock, D. G. Correlation of corn and soybean grain yield with topography and soil properties [J]. *Agronomy Journal*, 2000, 92(1): 75–83.

[11] Jiang, X. J., Xie, D. Combining ridge with no-tillage in lowland rice-based cropping system: long-term effect on soil and rice yield [J]. *Pedosphere*, 2009(4): 515–522.

[12] Wang, R., Jiang, Y., Su, P., *et al*. Global spatial distributions of and trends in rice exposure to high temperature [J]. *Sustainability*, 2019, 11: 6271.

[13] Tilman, D., Balzer, C., Hill, J., *et al*. Global food demand and the sustainable intensification of agriculture [J]. *Proceedings of the National Academy of Sciences of the United States of America*, 2011, 108(50): 20260–20264.

[14] Bijl, D. L., Bogaart, P. W., Dekker, S. C., *et al*. A physically-based model of long-term food demand [J]. *Global Environmental Change*, 2017, 45: 47–62.

[15] Watson, R. T., Zinyowera, M. C., Moss, R. H., Impacts, adaptations and mitigation of climate change: scientific-technical analyses [R]. Contribution of Working Group II to the Second Assessment Report of the Intergovernmental Panel on Climate Change, University Press, 1996.

[16] Taylor, K. E., Stouffer, R. J., Meehl, G. A. an overview of CMIP5 and the experiment design [J]. *Bulletin of the American Meteorological Society*, 2012, 93(4): 485–498.